J Fusion Energ (2012) 31:143–150
DOI 10.1007/s10894-011-9445-9

ORIGINAL RESEARCH

Dependence of Plasma Focus Argon Soft X-Ray Yield on Storage Energy, Total and Pinch Currents

M. Akel · S. Lee

Published online: 25 June 2011

Abstract Numerical experiments are carried out systematically to determine the argon soft X-Ray yield Y_{sxr} for optimized argon plasma focus with storage energy E_0 from 1 kJ to 1 MJ. The ratio c = b/a, of outer to inner radii; and the operating voltage V_0 are kept constant. E_0 is varied by changing the capacitance C_0. These numerical experiments were investigated on argon plasma focus at different operational gas pressures (0.41, 0.75, 1, 1.5, 2.5 and 3 Torr) for two different values of static inductance L_0 (270 and 10 nH). Scaling laws on argon soft X-Ray yield, in terms of storage energies E_0, peak discharge current I_{peak} and focus pinch current I_{pinch} were found. It was found that the argon X-ray yields scale well with $Y_{sxr} = 8 \times 10^{-11} I_{pinch}^{4.12}$ for the high inductance (270 nH) and $Y_{sxr} = 7 \times 10^{-13} I_{pinch}^{4.94}$ for the low inductance (10 nH), (where yields are in joules and current in kilo amperes). While the soft X-ray yield scaling laws in terms of storage energies were found to be as $Y_{sxr} = 0.05 \times E_0^{0.94}$ at energies in the 1–100 kJ region. The scaling 'drops' as E_0 is increased, and Y_{sxr} scales as $Y_{sxr} = 1.01 \times E_0^{0.33}$ at high energies towards 1 MJ for 10 nH at argon gas pressure of 1 Torr. The optimum efficiencies for SXR yield were found to be 0.00077% with a capacitor bank energy of 112.5 kJ for high inductance (270 nH) and 0.005% with a capacitor bank energy of 4.5 kJ for low inductance (10 nH). Therefore for larger devices, it may be necessary to operate at a higher voltage and use higher driver impedance to ensure increasing X-ray yield efficiency beyond the optimum values. As storage energy is changed the required electrode geometry for optimum yield is obtained and the resultant plasma pinch parameters are found. Required values of axial speed for argon soft X-ray emission were found to be in the range 11–14 cm/μs.

Keywords Plasma focus scaling laws · Soft X-ray scaling laws · Argon gas · Lee model

M. Akel (✉)
Department of Physics, Atomic Energy Commission,
P. O. Box 6091, Damascus, Syria
e-mail: pscientific@aec.org.sy

S. Lee
Institute for Plasma Focus Studies, 32 Oakpark Drive,
Chadstone, VIC 3148, Australia

S. Lee
National Institute of Education, Nanyang Technological
University, Singapore 637616, Singapore

S. Lee
INTI International University College, Nilai 71800, Malaysia

Introduction

Plasma focus devices have been studied as efficient, pulsed and intense sources of hard and soft X-rays with potential applications [1–3]. Whilst many recent experiments have concentrated efforts on low energy devices [1–3] with a view of operating these as repetitively pulsed sources, other experiments have looked at X-ray pulses from larger plasma focus devices [4, 5] extending to the megajoule regime. However, numerical experiments simulating X-ray pulses from plasma focus devices are gaining more interest in the public domain. For example, the Institute of Plasma Focus Studies [6] conducted an International Internet Workshop on Plasma Focus Numerical Experiments [7], at which it was demonstrated that the Lee model code [8] not only computes realistic focus pinch parameters, but also absolute values of SXR yield Ysxr which are consistent with those measured experimentally. A comparison was

made for the case of the NX2 machine [3], showing good agreement between computed and measured Ysxr as a function of operational pressure p_0 [7, 9]. This gives confidence that the Lee model code produces realistic results in the computation of Y_{sxr}. Numerical experiments are also carried out systematically by Lee et al. [10, 11] to determine the neon soft X-ray yield Y_{sxr} for optimized optimized conditions with storage energy E_0 from 1 kJ to 1 MJ. At each E_0, the optimum combination of P_0, z_0 and 'a' is found that produces the biggest Y_{sxr}. At low energies $Y_{sxr} \sim E_0^{1.6}$ whilst towards 1 MJ $Y_{sxr} \sim E_0^{0.8}$. The soft X-ray yield Y_{sxr} scaling laws are found to be $Y_{sxr} \sim I_{peak}^{3.2}$ (0.2 – 2.4 MA) and $Y_{sxr} \sim I_{pinch}^{3.6}$ (0.1–1.3 MA) throughout the range investigated. It also needs to be pointed out that the distinction of I_{pinch} from I_{peak} is of basic importance [12–14]. The scaling with I_{pinch} is the more fundamental and robust one, since obviously there are situations (no pinching or poor pinching however, optimized) where I_{peak} may be large but Y_{sxr} is zero or small, whereas the scaling with I_{pinch} is certainly more consistent with all situations. Gates, in optimization studies, had proposed [15] that the total energy emitted as X-rays may scale as $Y_x \sim I_{peak}^4 \big/ (\text{pinch radius})^2$. This scaling rule is not very useful for predictive purposes since for a given capacitor bank whilst I_{peak} may be estimated, the focus pinch radius is difficult to quantify. Moreover if one considers a certain gas, say, argon, then for an optimum operation one really needs to fix an axial speed, in which case the speed factor $S = \left(I_{peak}/a\right)/p_0^{0.5}$ (where a is the anode radius and p_0 is the operating pressure) is fixed [16]. Filippov et al. [5] reported a megajoule PF as an efficient X-ray source. In that work a 9.2 mF capacitor bank was charged up to 14 kV with energy storage of 0.9 MJ at 1 Torr neon. A fast plastic scintillator (0.2 mm thick NE 193) covered with 10 μm Al was used for X-ray detection. Ten percent of the capacitor bank energy was reported to convert into K-shell lines of Ne radiation. A scaling law $Y_x \sim I_{pinch}^{3.5-4}$ was proposed, where Y_x and I_p are the X-ray yield and the pinch current, respectively. Serban and Lee [17] investigated the soft X-ray emission from deuterium by employing filtered p-type intrinsic n-type (PIN) diodes. Scaling laws relating the soft X-ray yield to peak discharge current, peak axial velocity and anode radius were proposed. It was found that the X-ray yield varies as $Y_{sx} \sim I^n$ or $Y_{sx} \sim I^n v_{axial}^n$, where n = 2–4. They further reported that for a given operating pressure, the soft X-ray yield increases with the square of the axial speed in the range 7–14 cm/μs. However, it was described that the proposed scaling law was not so accurate. Sharif et al. [18] studied the Cu–Kα and total X-ray emissions from plasma focus with argon and hydrogen filling gases. It was found that Cu–Kα yield varies approximately following a scaling law: $Y_K[J] \sim [E(kJ)]^{3.5-4.5} \sim [I(100\,kA)]^{3.5-4.5}$, whereas the total X-ray emission was found to follow $Y_{tot}[J] \sim [E(kJ)]^{4.5-5.5} \sim [I(100kA)]^{4.5-5.5}$.

Sharif et al. [19] studied X-ray emissions from 2.3 to 5.3 kJ Mather-type plasma focus employing copper, molybdenum, and tungsten anode tip with argon filling gas. Characteristic Cu–Kα and Mo K-series emission and their ratio to the continuous X-ray are determined. From variation of the X-ray yield data with filling pressure at different charging voltages, scaling laws are obtained to be: that Cu–Kα yield varies approximately following a scaling law: $Y_K[J] \sim [E(kJ)]^{2.1-2.2} \sim [I(100\,kA)]^{2.9-3.3}$, whereas the total X-ray emission was found to follow $Y_{tot}[J] \sim [E(kJ)]^{2.8-3.7} \sim [I(100kA)]^{4.3-4.8}$ for copper anode with argon gas. For molybdenum insert at the anode tip with argon gas scaling law was found to be: $Y_K[J] \sim [E(kJ)]^{1.8-1.9} \sim [I(100\ kA)]^{2.4-3.0}$ for K radiation, whereas $Y_{tot}[J] \sim [E(kJ)]^{2.7-3.6} \sim [I(100kA)]^{4.2-4.6}$ for total x-radiation. In this work, scaling law for tungsten insert at anode tip with hydrogen gas was also found to be: $Y_{tot}[J] \sim [E(kJ)]^{2.4-2.5} \sim [I(100kA)]^{3.3-3.9}$ for total x-radiation. Zakaullah et al. [20, 21] studied the X-radiation emission from a low energy plasma focus with argon as a filling gas. Specifically, the attention is paid to determine the system efficiency for argon K-lines and Cu–K line emission at different filling pressures, and identify the radiation emission region. The highest argon line emission found at 1.5 mbar is about 30 mJ and the corresponding efficiency is 0.0015%. Wong et al. [22] studied the emission characteristics of a high-performance low-energy (3-kJ) repetitive dense plasma focus device, NX2, operated at up to 1-Hz repetition rate to develop it as an intense source of soft X-rays (SXR) for microlithography and micromachining. Various SXR yield optimization studies with argon and neon as filling gases were performed under different operating conditions (charging voltage, filling pressure, anode length, and insulator sleeve length). The SXR yield was computed using signals obtained from a PIN diode SXR spectrometer with appropriate filters. When operated in neon, the average optimum SXR (1 nm) yield in 4 steradians was found to be up to 140 J/shot, which corresponded to a wall plug efficiency of 5.6%. Operation in argon showed that optimized SXR (0.4 nm) yield was up to 1.3 J/shot.

In the context of soft X-ray argon scaling law over any significant range of energies, no experimental or numerical work appears to have been reported in the literature. In this paper, we show the comprehensive range of numerical experiments conducted to derive scaling laws on argon soft X-ray yield, in terms of storage energies E_0, peak discharge current I_{peak} and focus pinch current I_{pinch} obtained from studies carried out over storage energies E_0 varying

from 1 kJ to 1 MJ for optimized plasma focus device parameters.

The Lee Model Code for Argon Soft X-ray Yields

The Lee model couples the electrical circuit with plasma focus dynamics, thermodynamics and radiation, enabling realistic simulation of all gross focus properties. This approach focusing on gross properties is different from magnetohydrodynamic (MHD) codes where spatially resolved and detailed description of plasma properties is calculated. Many authors have developed and used MHD and fluid models of the plasma focus. Behler and Bruhns [23] developed a 2D three-fluid code. Garanin and Mamyshev [24] introduced the MHD model, which takes into account anomalous resistivity. However, none of these studies [23–28] has resulted in published data on SXR yields, nor any comparison with laboratory experiments on SXR yields [23–28]. Our basic model, described in 1984 [29], was successfully used to assist several projects [30–32]. Radiation-coupled dynamics was included in the five-phase code leading to numerical experiments on radiation cooling [33]. The vital role of a finite small disturbance speed discussed by Potter in a *Z*-pinch situation [34] was incorporated together with real gas thermodynamics and radiation-yield terms. Before this 'communication delay effect' was incorporated, the model consistently over-estimated the radial speeds by a factor of ~ 2 and shock temperatures by a factor ~ 4. This version, using the 'signal-delay slug', which became a must-have feature in all subsequent versions, assisted other research projects [35–38] and was web-published in 2000 [39] and 2005 [40]. Plasma self-absorption was included in 2007 [39] improving SXR yield simulation. The code has been used extensively in several machines including UNU/ICTP PFF [30, 33, 35, 36, 41–43], NX2 [3, 37, 38], NX1 [2, 3] and adapted for the Filippov-type plasma focus DENA [44]. A recent development is the inclusion of the neutron yield, *Yn*, using a beam–target mechanism [13, 45–48], incorporated in recent versions [8] of the code (later than RADPFV5.13), resulting in realistic Yn scaling with I_{pinch} [45, 46]. The versatility and the utility of the model are demonstrated in its clear distinction of I_{pinch} from I_{peak} [12] and the recent uncovering of a plasma focus pinch current limitation effect [13, 14]. The Lee model was modified to include nitrogen and oxygen, and it was used to characterization and soft X-ray optimization from nitrogen and oxygen plasma focus [49–51]. The description, theory, code and a broad range of results of this 'Universal Plasma Focus Laboratory Facility' are available for download from [8, 52]. In the code, argon line radiation Q_L is calculated as follows:

$$\frac{dQ_L}{dt} = -4.6 \times 10^{-31} N_i^2 Z_{eff} Z_n^4 (\pi a_{min}^2) Z_{max} / T$$

where for the temperatures of interest in our experiments we take $Ysxr = Q_L$.

Hence the SXR energy generated within the plasma pinch depends on the following properties: number density N_i, effective charge number Z_{eff}, atomic number of gas Z_n, pinch radius a_{min}, pinch length Z_{max}, plasma temperature T and the pinch duration. This generated energy is then reduced by the plasma self-absorption which depends primarily on density and temperature; the reduced quantity of energy is then emitted as the soft X-ray yield. From the reported experimental results [37, 42], the X-ray emissions from argon plasma are mainly He-like alpha line (He_α ($1s^2$-1s2p, Ar: 3.9488 A^o or 3,140 eV)) and H-like alpha line (Ly_α (1s-2p, Ar: 3.731 A^o or 3,323 eV) lines. So the most intense characteristic emissions of argon plasma are Ly_α and He_α lines. The corresponding X-ray emitters in the argon plasmas are mainly H-like and He-like ions. It is shown that for operation in argon, a focus pinch compression temperature of 1.4–5 keV (16.3×10^6–58.14×10^6 K) is suitable for generating H-like and He-like ions in argon plasma (therefore argon soft X-ray emissions) [37]. This also agrees with the reported temperature measurements with X-ray radiative argon plasma (1.8 keV [53], 1.4–2.4 keV [54], 1–5 keV [55], 1.5–2.5 keV [56]), in which the argon plasma was working around its temperature regime for X-ray output. Hence unlike the case of neutron scaling, for SXR scaling there is an optimum small range of temperatures (*T* window) in which to operate. In the modified Lee model code version RADPF5.15 K, we take the argon soft X-ray yield (generation H-like and He-like ions) to be equivalent to line radiation yield i.e. $Y_{sxr} = Q_L$ at the following temperature range 1.4–5 keV.

Numerical Experiments: Results and Discussion

We use the Lee model code to carry out a series of numerical experiments over the energy range 1 kJ–1 MJ. For argon operation, the Lee model code had previously been designed to compute the line radiation yield. For this work we want to distinguish that part of the line yield that is soft X-rays. Reviewing previous experimental and numerical work by Liu [42] and more detailed numerical work by Shan Bing [37] we are able to fix a temperature range for argon at which the radiation is predominantly soft X-ray coming from He-like and H-like argon ions. Shan Bing in particular carried out a line-by-line computation using a corona method and computed the relative intensities of each of four argon soft X-ray lines (He- and H-like)

as functions of temperature. From this review we set the following temperature range: (16.3×10^6–58.14×10^6 K) as that relevant to the production of argon soft X-rays. In any shot, for the duration of the focus pinch, whenever the focus pinch temperature is within this range, the line radiation is counted as argon soft X-rays. Whenever the pinch temperature is outside this range, the line radiation is not included as argon soft X-rays.

During all our numerical experiments, the following parameters are kept constant: the ratio b = c/a (kept at 3.368) and the operating voltage V_0 (kept at 15 kV), the ratio of stray resistance to surge impedance RESF (kept at 0.337). The model parameters [7, 8, 10–14] f_m, f_c, f_{mr}, f_{cr} are also kept at fixed suitable values of 0.05, 0.7, 0.15 and 0.7 for our AECS-PF2 device [57], with argon filling gas [58]. The numerical experiments are also investigated at two different static inductance values L_0: the first is the high inductance of 270 nH, corresponding to fitting procedures of calculated and experimental current traces of AECS-PF2 for argon gas at operational pressure of 0.41 Torr. While the second one is low inductance 10 nH, at which the pinch current limitation effect of argon plasma focus was obtained.

The storage energy E_0 is changed (from 1 kJ to 1 MJ) by changing the capacitance C_0 (from 10 μF up to 9,000 μF). Parameters that are varied are anode length z_0 and anode radius 'a', operating pressure p_0. Parametric variation at each E_0 follows the anode length z_0 and 'a' until all realistic combinations of E_0, z_0 and 'a' are investigated. At each E_0, the optimum combination of z_0 and 'a' is found that produces the biggest Y_{sxr}. In other words at each E_0, a p_0 is fixed, a z_0 is chosen and 'a' is varied until the largest Y_{sxr} is found. This procedure is repeated until for that E_0 the optimum combination of z_0 and 'a' is found. Then keeping the same values of E_0, another p_0 is selected. The procedure for parametric variation of z_0 and 'a' as described above is then carried out for this E_0 and new p_0 until the optimum combination of z_0 and 'a' is found. In this manner, numerical experiments were investigated on argon plasma focus at different operational gas pressures (0.41, 0.75, 1, 1.5, 2.5 and 3 Torr) for two different static inductance values L_0 (270 and 10 nH) and then after systematically carrying out more than 3,000 shots, the optimized shots for various energies are obtained. Tables 1 and 2 show optimized configuration found for each E_0 for 270 and 10 nH at gas pressure of 1 Torr, respectively. From the data of Table 1, we plot Y_{sxr} against E_0 as shown in Fig. 1. From Fig. 1 we found that Y_{sxr} scales as $Y_{sxr} = 7 \times 10^{-4} E_0^{1.55}$ at energies in the 1–100 kJ regions. The scaling 'drops' as E_0 is increased, and Y_{sxr} scales as $Y_{sxr} = 229 \times 10^{-4} E_0^{0.77}$ at high energies towards 1 MJ. We then plot Y_{sxr} against I_{peak} and I_{pinch} and obtain Fig. 2, which shows that $Y_{sxr} = 8 \times 10^{-11} I_{pinch}^{4.12}$ and $Y_{sxr} = 2 \times 10^{-11} I_{peak}^{4.1}$. From the data of Table 2, we also plot Y_{sxr} against E_0 as shown in Fig. 3. From Fig. 3 we found that Y_{sxr} scales as $Y_{sxr} = 0.05 \times E_0^{0.94}$ at energies in the 1–100 kJ regions. The scaling also 'drops' as E_0 is increased, and Y_{sxr} scales as $Y_{sxr} = 0.32 \times E_0^{0.52}$ and $Y_{sxr} = 1.01 \times E_0^{0.33}$ at high energies towards 1 MJ. We then plot Y_{sxr} against I_{peak} and I_{pinch} and obtain Fig. 4, which shows that $Y_{sxr} = 7 \times 10^{-13} I_{pinch}^{4.94}$ and $Y_{sxr} = 2 \times 10^{-15} I_{peak}^{5.47}$.

The resulting Y_{sxr} versus I_{pinch} and I_{peak} log–log curves remains a straight line, with the scaling index 4.12 and 4.1, respectively at high inductance (Fig. 3), while the resulting

Table 1 Optimised configuration found for each E_0

E_0 (kJ)	C_0 (μF)	a (cm)	z_0 (cm)	I_{peak} (kA)	I_{pinch} (kA)	v_a (cm/μs)	Y_{sxr} (J)	Efficiency (%)
1.1	10	0.23	15	66.9	46.7	10.9	0.0006	0.000055
2.8	25	0.34	23	101.7	70.8	10.9	0.0034	0.00012
4.5	40	0.42	31	125.1	87.0	11.0	0.0077	0.00017
5.6	50	0.46	35	138.0	96.0	11.0	0.0116	0.0002
11.3	100	0.61	43	183.1	127.2	10.9	0.0359	0.00032
22.5	200	0.80	59	239.1	165.8	11.0	0.1049	0.00047
45.0	400	1.02	91	305.4	211.5	11.2	0.2832	0.00063
67.5	600	1.16	99	346.5	239.8	11.1	0.4717	0.0007
90.0	800	1.26	115	377.2	261.0	11.2	0.6565	0.00073
112.5	1,000	1.34	123	400.7	277.2	11.2	0.8623	0.00077
450.0	4,000	1.70	131	510.8	352.5	10.9	2.5561	0.00057
900.0	8,000	1.85	147	556.5	383.8	10.9	3.9001	0.00043
1,012.5	9,000	1.97	199	592.6	409.1	11.2	5.1121	0.0005

Optimization carried out with $RESF = 0.337$, $c = 3.368$, $L_0 = 270$ nH and $V_0 = 15$ kV and model parameters f_m, f_c, f_{mr}, f_{cr} are fixed at 0.05, 0.7, 0.15 and 0.7, respectively, v_a is the peak axial speed at 1 Torr

Table 2 Optimized configuration found for each E_0

E_0 (kJ)	C_0 (μF)	a (cm)	z_0 (cm)	I_{peak} (kA)	I_{pinch} (kA)	v_a (cm/μs)	Y_{sxr} (J)	Efficiency (%)
1.1	10	0.70	4	251.4	148.8	13.60	0.05	0.0045
2.8	25	0.90	6	329.5	193.1	13.98	0.13	0.0046
4.5	40	1.01	8	370.7	217.1	14.08	0.22	0.0048
5.6	50	1.07	9	390.4	229.0	14.08	0.26	0.0046
11.3	100	1.24	15	448.8	264.3	14.03	0.52	0.0046
22.5	200	1.41	23	503.5	300.1	13.79	1.01	0.0045
45.0	400	1.58	37	551.9	333.6	13.46	1.85	0.0041
67.5	600	1.68	43	578.3	354.5	13.30	2.52	0.0037
90.0	800	1.74	57	594.5	366.1	13.11	3.15	0.0035
112.5	1,000	1.80	61	607.3	377.2	13.03	3.72	0.0033
450.0	4,000	2.07	133	669.8	432.4	12.48	7.67	0.002
900.0	8,000	2.18	177	692.4	454.9	12.30	9.66	0.001
1,012.5	9,000	2.20	209	695.7	457.8	12.24	10.03	0.0001

Optimization carried out with RESF = 0.337, c = 3.368, L_0 = 10 nH and V_0 = 15 kV and model parameters f_m, f_c, f_{mr}, f_{cr} are fixed at 0.05, 0.7, 0.15 and 0.7, respectively, v_a is the peak axial speed at 1 Torr

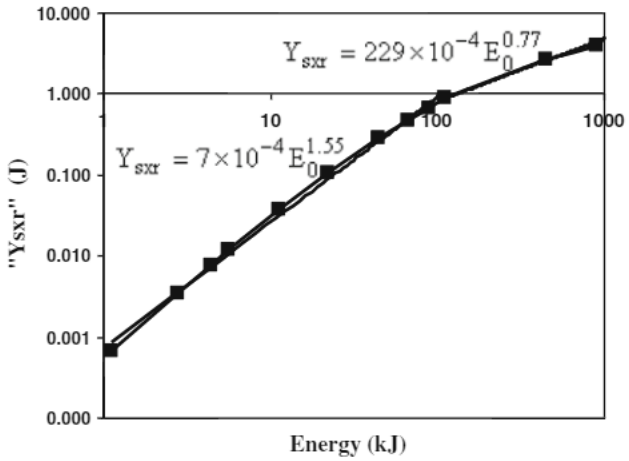

Fig. 1 Y_{sxr} versus E_0. The parameters kept constants are: RESF = 0.337, c = 3.368, L_0 = 270 nH, p_0 = 1 Torr and V_0 = 15 kV and model parameters f_m, f_c, f_{mr}, f_{cr} at 0.05, 0.7, 0.15 and 0.7, respectively

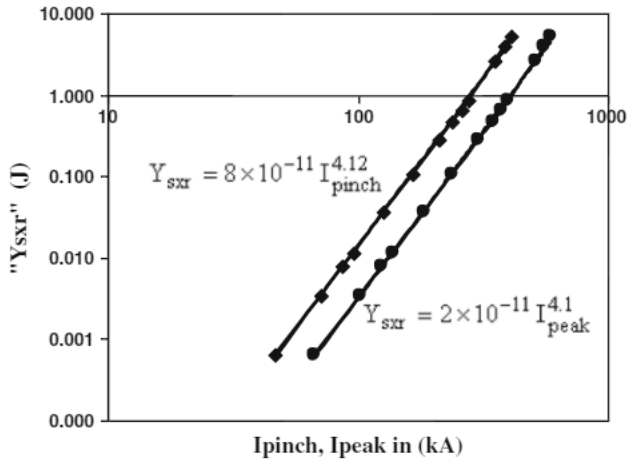

Fig. 2 Y_{sxr} versus I_{pinch}, I_{peak}. The parameters kept constants are: RESF = 0.337, c = 3.368, L_0 = 270nH, p_0 = 1 Torr and V_0 = 15 kV and model parameters f_m, f_c, f_{mr}, f_{cr} at 0.05, 0.7, 0.15 and 0.7, respectively

Y_{sxr} versus I_{pinch} and I_{peak} log–log curves found to be with the scaling index 4.94 and 5.47, respectively, at low inductance (Fig. 4). From Fig. 4 it can be seen that the resulting Y_{sxr} versus I_{peak} log–log curve is larger scatter than Y_{sxr} versus I_{pinch} log–log curve.

Another way of looking at the comparison of the I_{pinch} scaling and the I_{peak} scaling is to consider some unoptimised cases e.g. at very high or very low pressures. In these cases, Y_{sxr} is zero and I_{pinch} is zero but there is a value for I_{peak}. This is an argument that the I_{pinch} scaling is more robust. However, it must be noted that both scaling are applicable only to optimized points. Nevertheless noting that the $Y_{sxr} \sim I_{pinch}$ scaling has less scatter than the $Y_{sxr} \sim I_{peak}$ scaling, the conclusion is that the I_{pinch} scaling is the more universal and robust one. Tables 1 and 2 show that the electrode geometry increases with increasing the storage energy from 1 kJ to 1 MJ, while it is noticed that the peak axial speed suitable for maximum argon soft X-ray yield changes slightly over this wide energy range, this means that there is a required range of axial speed in plasma focus devices for argon soft X-ray emission, for example, in our case these values are in the range 11–14 cm/μs. Figure 5 illustrates variations of the electrode geometry and the optimum peak axial speed versus storage energy for L_0 = 10 nH at 1 Torr. These numerical experiments with argon plasma focus over storage energy range of 1 kJ–1 MJ show that within the stated constraints

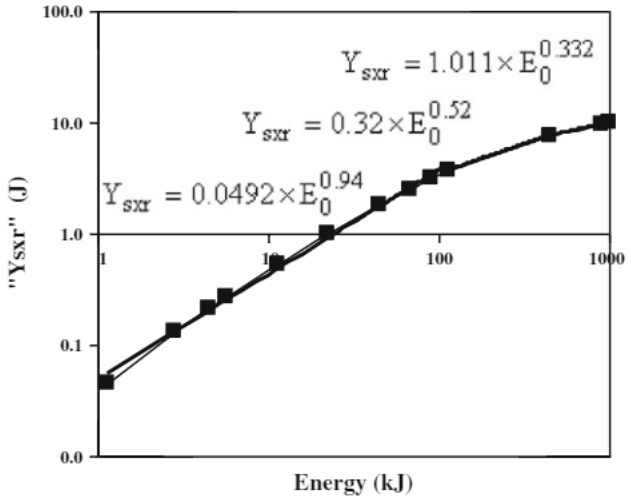

Fig. 3 Y_{sxr} versus E_0. The parameters kept constants are: RESF = 0.337, c = 3.368, L_0 = 10nH, p_0 = 1 Torr and V_0 = 15 kV and model parameters f_m, f_c, f_{mr}, f_{cr} at 0.05, 0.7, 0.15 and 0.7, respectively

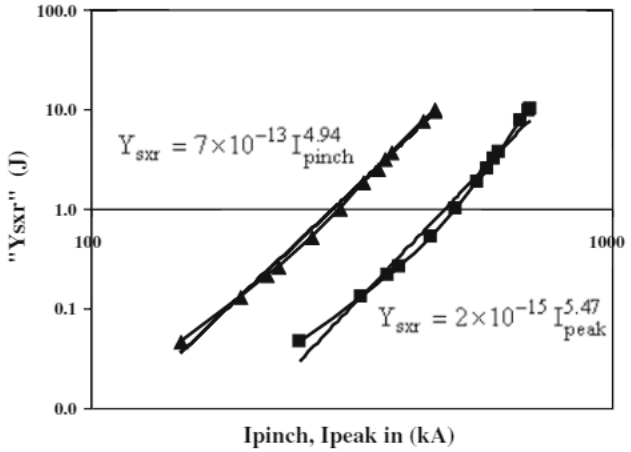

Fig. 4 Y_{sxr} versus I_{pinch}, I_{peak}. The parameters kept constants are: RESF = 0.337, c = 3.368, L_0 = 10nH, p_0 = 1 Torr and V_0 = 15 kV and model parameters f_m, f_c, f_{mr}, f_{cr} at 0.05, 0.7, 0.15 and 0.7, respectively

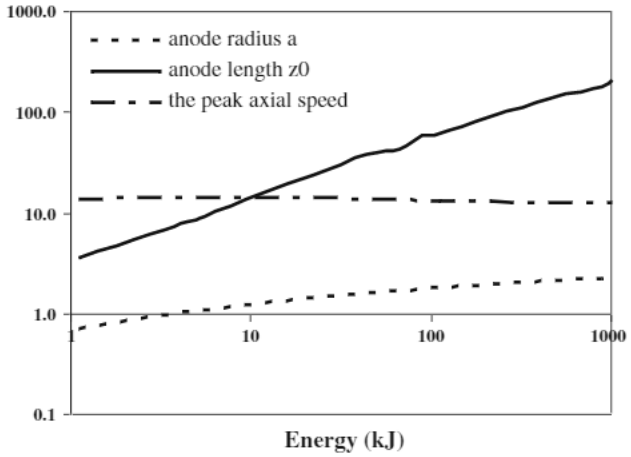

Fig. 5 Variations of the electrode geometry and the optimum peak axial speed versus storage energy for L_0 = 10 nH at 1 Torr of pressure

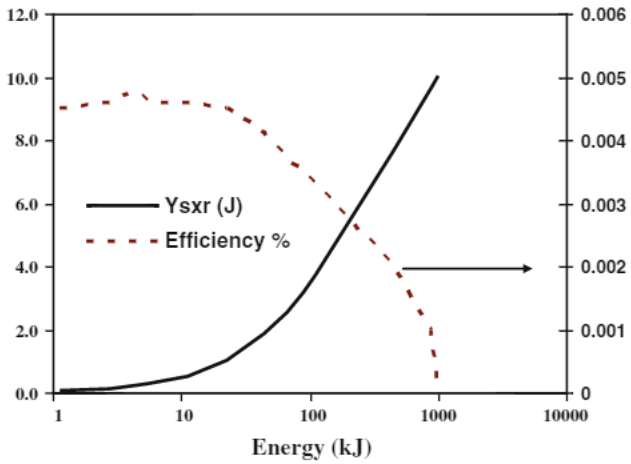

Fig. 6 Argon soft X-ray yield and the optimum efficiency versus storage energy for L_0 = 10 nH at 1 Torr of pressure

of these experiments, scaling with E_0 decreases towards the high energy range 1 MJ. A single power law applies for each of I_{peak} and I_{pinch} scaling laws. The observations of the numerical experiments, bolstered by fundamental considerations is that the I_{pinch} scaling is the more universal and robust one. This implies that for applications requiring high X-ray yield, the plasma focus must be designed to optimize I_{pinch}. For example from Table 1, it can be seen that the optimum efficiency for SXR yield (0.00077%) is with a capacitor bank energy of 112.5 kJ and from Table 2, it can be seen that the optimum efficiency for SXR yield (0.005%) is with a capacitor bank energy of 4.5 kJ (see Fig. 6). One factor may be that beyond these optimum energies, I_{pinch} do not increase well with bank energy due to the increase in the impedance of the plasma focus in comparison with that of the bank impedance. Therefore for larger devices, it may be necessary to operate at a higher voltage and use higher driver impedance to ensure increasing X-ray yield efficiency. Based on the scaling law proposed here, it is possible to classify experimental yield enhancements into three categories: (i) 'compensating for unoptimized focus' where experiments start off with a focus showing unexpectedly low yield, i.e. below the scaling law and then the yield is 'enhanced' by techniques other than changing of anode dimensions to follow the scaling law, (ii) 'increasing I_{pinch}' for example by reducing the current shedding or increasing the current by current

stepping with novel driver circuits where the enhanced device still follows the same scaling law and (iii) 'new regime of operation' where plasma parameters such as density, dimensions and lifetime are changed at the same I_{pinch} and yield is beyond the scaling law.

Conclusions

Numerical experiments were investigated on argon plasma focus at different operational gas pressures (0.41, 0.75, 1, 1.5, 2.5 and 3 Torr) for two different static inductance values L_0 (270 and 10 nH). In conclusion, this report has shown that within the scope of this report, argon X-ray yields scale well with $Y_{sxr} = 8 \times 10^{-11} I_{pinch}^{4.12}$ for the high inductance (270 nH) and $Y_{sxr} = 7 \times 10^{-13} I_{pinch}^{4.94}$ for the low inductance (10 nH), (where yields are in joules and current in kilo amperes). These numerical experiments confirm that the Y_{sxr} versus I_{pinch} scaling is more robust and universal.

The soft X-ray yield scaling laws in terms of storage energies were also derived, and it was found that the scaling drops as E_0 (in kJ) is increased.

This implies that for applications requiring high X-ray yield, the plasma focus must be designed to optimize I_{pinch}. The optimum efficiencies for SXR yield were found to be 0.00077% with a capacitor bank energy of 112.5 kJ for high inductance (270 nH) and 0.005% with a capacitor bank energy of 4.5 kJ for low inductance (10 nH). Therefore for larger devices, it may be necessary to operate at a higher voltage and use higher driver impedance to ensure increasing X-ray yield efficiency beyond the optimum values.

The influence of storage energy on the electrode geometry, the plasma focus parameters, argon soft X-ray yield and efficiency has been studied. Required values of axial speed in plasma focus devices for argon soft X-ray emission were found to be in the range 11–14 cm/μs. As seen in our numerical experiments such high values of axial speed require larger than normal Ipeak/a of more than 300kA/cm. If we consider an upper limit of Ipeak/a of 360kA, then we may consider as feasible the scaling that we have done at 1 Torr, since the value of Ipeak/a for 1 Torr Argon reaches just about this upper limit value. For pressure greater than 1 Torr, the required Ipeak/a exceeds this upper limit of Ipeak/a. For that reason in this paper we deal only with scaling for 1 Torr.

Acknowledgments The authors would like to thank Director General of AECS, for encouragement and permanent support. The authors would also like to express thanks to Prof. Dr. Sharif Al-Hawat, who provide us with experimental current traces of argon AECS PF-2. M. Akel would also like to express thanks to Mrs. Sheren Isamael, who collaborated going through all the numerical experiments using Lee Model.

References

1. Y. Kato, S.H. Be, Appl. Phys. Lett. **48**, 686 (1986)
2. E.P. Bogolyubov et al., Phys. Scr. **57**, 488–494 (1998)
3. S. Lee et al., IEEE Trans. Plasma Sci. **26**, 1119 (1998)
4. N.V. Filippov et al., IEEE Trans. Plasma Sci. **24**, 1215–1223 (1996)
5. N.V. Filippov et al., Phys. Lett. A **211**, 168–171 (1996)
6. Institute for plasma focus studies http://www.plasmafocus.net
7. Internet workshop on plasma focus numerical experiments (IPFS-IBC1), 14 April–19 May (2008)
8. S. Lee, "Radiative dense plasma focus computation package: RADPF", http://www.intimal.edu.my/school/fas/UFLF/. http://www.plasmafocus.net/IPFS/modelpackage/File1RADPF.htm, (2011)
9. S. Lee et al., J. Appl. Phys. **106**, 023309 (2009)
10. S. Lee et al., Plasma Phys. Control Fusion, **51**, 105013, (8 pp) (2009)
11. S. H. Saw, S. Lee, Energ. Power Eng. **2**(1), 65–72 (2010)
12. S. Lee et al., Appl. Phys. Lett. **92**, 111501 (2008)
13. S. Lee et al., Appl. Phys. Lett. **92**, 021503 (2008)
14. S. Lee et al., Plasma Phys. Control Fusion **50**, 065012 (2008)
15. D.C. Gates, *Proceedings 2nd International Conference on Energy Storage, Compression and Switching (Venice, Italy, 1978)*, vol. 2 (New York: Plenum) p 329 (1983)
16. S. Lee et al., IEEE Trans. Plasma Sci. **24**, 1101 (1996)
17. A. Serban et al., Plasma Sources Sci. Technol. **6**, 78 (1997)
18. M. Sharif et al., Plasma Sources Sci. Technol. **13**, B7–B13 (2004)
19. M. Sharif et al., J. Appl. Phys. **100**, 073301 (2006)
20. M. Zakaullah et al., IEEE Trans. Plasma Sci. **30**, 6, 2089 (2002)
21. M. Zakaullah et al., Plasma Sources Sci. Technol. **9**, 592–596 (2000)
22. D. Wong et al., IEEE Trans. Plasma Sci. **32**, 6 (2004)
23. K. Behler, H. Bruhns, Phys. Fluids **30**, 3767 (1987)
24. S.F. Garanin, V.I. Mamyshev, Plasma Phys. Rep. **34**, 639–649 (2008)
25. D.E. Potter, Phys. Fluids **14**, 1911 (1971)
26. V. Vikhrev et al., Nucl. Fusion **33**, 311 (1993)
27. W. Stepniewski, J. Phys.: Conf. Ser. **44**, 215–220 (2006), doi: 10.1088/1742-6596/44/1/031 (1st Int. Workshop and Summer School on Plasma Physics (IWSSPP'05) (Kiten, Bulgaria, 8–12 June 2005))
28. V. Yordanov et al., J. Phys.: Conf. Ser. **44**, 15–20, (2006), doi: 10.1088/1742-6596/44/1/031 (1st Int. Workshop and Summer School on Plasma Physics (IWSSPP'05)(Kiten, Bulgaria, 8–12 June 2005))
29. S. Lee, Plasma focus model yielding trajectory and structure Radiations in Plasmas vol. II ed B McNamara (Singapore: World Scientific) ISBN 9971-966-37-9, pp 978–87 (1984)
30. S. Lee et al., Am. J. Phys. **56**, 62 (1988)
31. T.Y. Tou et al., IEEE Trans. Plasma Sci. **17**, 311 (1989)
32. S. Lee, IEEE Trans. Plasma Sci. **19**, 912 (1991)
33. J.b. Ali, Development and studies of a small plasma focus PhD Thesis Universiti Teknologi Malaysia, Malaysia, (1990)
34. D.E. Potter, Nucl. Fusion **18**, 813–823 (1978)
35. S. Lee, A. Serban, J. Plasma Phys. **60**, 3–15 (1998)
36. M.H. Liu et al., IEEE Trans. Plasma Sci. **26**, 135–140 (1998)
37. S. Bing, Plasma dynamics and X-ray emission of the plasma focus PhD Thesis NIE ICTP Open Access Archive: http://eprints.ictp.it/99/ (2000)
38. D. Wong et al., Plasma Sources Sci. Technol. **16**, 116–23 (2007)
39. S. Lee, http://ckplee.myplace.nie.edu.sg/plasmaphysics/ (2000–2007)
40. S. Lee, ICTP Open Access Archive: http://eprints.ictp.it/85/ (2005)

41. S. Lee, Twelve Years of UNU/ICTP PFF—A Review IC 98 (231) Abdus Salam ICTP, Miramare, Trieste; ICTP OAA: http://eprints.ictp.it/31/ (1998)
42. M. Liu, Soft X-rays from compact plasma focus PhD Thesis Nanyang Technological University Singapore. ICTP Open Access Archive: http://eprints.ictp.it/327/ (1996)
43. S.H. Saw et al., IEEE Trans. Plasma Sci. **37**, 1276–1282 (2009)
44. V. Siahpoush et al., Plasma Phys. Control Fusion, **47**, 1065 (2005)
45. S. Lee, S.H. Saw, J. Fusion Energ. **27**, 292–295 (2008)
46. S. Lee, Plasma Phys. Control Fusion **50**, 105005 (2008)
47. V.A. Gribkov et al., J. Phys. D Appl. Phys. **40**, 3592 (2007)
48. S.V. Springham et al., Plasma Phys. Control Fusion, **42**, 1023, (2000)
49. M. Akel, Sh. Al-Hawat, S. Lee, J. Fusion Energ. **28**, 4, 355–363 (2009)
50. M. Akel, Sh. Al-Hawat, S. Lee, J. Fusion Energ. **29**, 1, 94 (2010)
51. M. Akel et al., J. Fusion Energ. **29**, 223–231 (2010)
52. M. Akel, Sh. Al-Hawat, S. Lee, J. Fusion Energ. **30**, 1, 39–47 (2011)
53. T. Yanagidaira et al., J. Phys. Soc. Jpn. **68**, 852–856 (1999)
54. S.R. Mohanty et al., Phys. Lett. A **234**, 472–476 (1997)
55. S.P. Moo, C.S. Wong, A.C. Chew, S. Lee, 12 years of research and training with the UNU/ICTP PFF at the university of Malaya, in Twelve Years of UNU/ICTP PFF – A Review (1998)
56. Sh. Al-Hawat, M. Akel, C.S. Wong, J. Fusion Energ. DOI 10.1007/s10894-011- 9417-0 (2011)
57. Sh. Al-Hawat, M. Akel, S. Lee, J. Fusion Energ. DOI 10.1007/s10894-011-9416-1 (2011)
58. Sh. Al-Hawat, M. Akel, S. Lee, S.H. Saw, J. Fusion Energ. DOI 10.1007/s10894-011-9414-3 (2011)